Kibble-Zurek mechanism in a topological phase transition

Minchul Lee

Department of Applied Physics and Institute of Natural Science, College of Applied Science, Kyung Hee University, Yongin 446-701, Korea

Seungju Han

Department of Physics, Korea University, Seoul 136-701, Korea

Mahn-Soo Choi[*]

Department of Physics, Korea University, Seoul 136-701, Korea

The Kibble-Zurek mechanism (KZM) is generalized to a class of multilevel systems and applied to study the quenching dynamics of one-dimensional (1D) topological superconductors (TS) with open ends. Unlike the periodic boundary condition, the open boundary condition, which is crucial for the zero-mode Majorana states localized at the boundaries, requires one to consider many coupled levels. Our generalized KZM predictions agree well with the numerically exact results for the 1D TS. In particular, the generalized KZM explains well the Majorana-mode contribution to the topological defects, which utterly defies the traditional KZM. The inherent bound-state character and multilevel structure of the Majorana mode, which play key roles in the TS, are efficiently captured by the generalized KZM.

I. INTRODUCTION

Conventional second-order phase transitions (PTs) are driven by the spontaneous symmetry breaking and typically described by local order parameters, which take continuous values. Various critical scalings are traced back to symmetry breaking. On the contrary, topological PTs involve the change in internal topology rather than symmetry breaking. Necessarily, topological states are classified by topological quantum numbers, which are discrete. For instance, topological insulators and superconductors are characterized by the number of gapless boundary (surface, edge, or endpoint) states [1–3] separated from gapped bulk states. These observations raise an intriguing question of how the topological order emerges or disappears temporally when system parameters are quenched across the critical point [4–7].

This question becomes even more curious when one recalls that the Kibble-Zurek mechanism (KZM), i.e., a theory of the formation of topological defects in second-order PTs, establishes quite accurate connections between the equilibrium critical scalings and the nonequilibrium dynamics of symmetry breaking. The KZM was originally put forward to study the cosmological PT of the early universe [8,9] and later extended to study classical PTs in condensed matter [10,11]. Recently, it was found to apply to the Landau-Zener transitions in two-level quantum systems [12,13] and the dynamics of second-order quantum PTs [14,15] as well. In fact, these latter two classes of dynamics share a key characteristic, the "critical slowing down" which comes from the critical scaling of the correlation length for the former and the reduced level spacing for the latter. Nevertheless, the agreement between the KZM prediction and the exact dynamics still remains "somewhat surprising" [16]. It is then a demanding question of whether topological PTs, which are not even driven by symmetry

breaking (critical scaling), can be described in the spirit of KZM. Interestingly, a recent study of the Creutz ladder and the *p*-wave superconductor wire pointed out that topology makes the density of defects deviate strongly from the *two-level* KZM scaling [6,7].

In this work, we generalize the KZM to a class of multilevel systems and apply it to study the quenching dynamics of one-dimensional (1D) topological superconductors (TS). We stress that the open boundary condition (OBC), which is crucial for the zero-mode Majorana states localized at the boundaries, requires us to consider many coupled levels [6,17]. Under the periodic boundary condition (PBC), the system is essentially a two-level system involving two modes of opposite momenta [14,18]. The traditional KZM has been thus limited to effectively two-level systems by adopting the periodic boundary condition or by considering only the low-lying two levels in the open-end systems. To extend the KZM to multilevel systems, we formulate the dynamics using the dynamical transition matrix and develop the so-called conserving and nonconserving KZM. Both are equivalent to the KZM for two-level systems. Our generalized KZM predictions, taking into account the Majorana states formed at its ends and its dynamical transition into multilevels, agree well with the numerically exact results for the 1D TS, capturing the inherent bound-state character and multilevel transition behavior of the Majorana mode. Our approach may provide a systematic and efficient way to understand the time evolution of more general classes of systems beyond two-level systems.

II. GENERALIZED KIBBLE-ZUREK MECHANISM

We first state the dynamical problem of our concern and develop the generalized KZM to attack the problem. Since the many-body dynamics of a noninteracting system is closely related to the single-particle dynamics, we focus on the single-particle dynamics here. We will come back to the full many-body problem in the following sections.

---

*choims@korea.ac.kr

Consider a single-particle Hamiltonian $H(t)$ which varies with time t via a time-dependent parameter $M(t)$ and defines $(N + 1)$ instantaneous eigenstates $|\Phi_n(t)\rangle$ with energies $E_n(t)$ $(n = 0, 1, \ldots, N;\ N = \infty$ for the continuum model) at each time t. When $|\Psi(t)\rangle$ is expanded into $|\Psi(t)\rangle = \sum_n \beta_n(t)|\Phi_n(t)\rangle$, the amplitudes $\beta_n(t)$ satisfy the effective Schrödinger equation,

$$i\frac{d}{dt}\beta_m(t) = \sum_n K_{mn}(t)\beta_n(t), \tag{1}$$

with $K_{mn}(t) \equiv \delta_{mn}E_n(t) - \Omega_{mn}(t)$ and $\Omega_{mn}(t) \equiv i\langle\Phi_m(t)|\dot{\Phi}_n(t)\rangle$ or, equivalently,

$$\beta_m(t) = \sum_n U_{mn}(t, t_0)\beta_n(t_0). \tag{2}$$

The effective Hamiltonian $K(t)$ in (1) includes off-diagonal elements $\Omega_{mn}(t)$ with the common phase fixing choice $\Omega_{nn}(t) = 0$. Mathematically, the matrix $\Omega(t)$ gives the *dynamical connection* between the instantaneous eigenstates at different times, $\langle\Phi_m(t)|\Phi_n(t')\rangle = W_{mn}(t, t') \equiv T\exp[i\int_{t'}^t ds\,\Omega(s)]$. Physically, $\Omega_{mn}(t)$ is responsible for the *dynamical transitions* between different instantaneous energy levels $E_m(t)$ and $E_n(t)$.

The essential spirit of the KZM is to devise an efficient method to examine the true dynamical wave function $|\Psi(t)\rangle$ of the system based on the adiabatic-impulse approximation. Hence it requires the intrinsic time scales of the system to all be known. The simplest is the case where all instantaneous eigenstates are known, as we primarily discuss in the present work. It is stressed that calculating *instantaneous* eigenstates is usually simple and easy, whereas solving true dynamics [Eqs. (1) or (2)] out of such instantaneous eigenstates can often be very complicated and difficult. For example, even a single spin 1/2 under a time-dependent external magnetic field cannot be solved exactly in general (except for the Rabi and Landau-Zener models). In this respect, our scheme cannot apply directly to topological states involving strong many-body correlation. In order for our scheme to be applied to such correlation-induced topological states, some approximate quasiparticle spectrum needs to be available.

The generalized KZM to be developed below requires the energy levels $E_n(t)$ and the dynamical transitions $\Omega_{mn}(t)$ between them to satisfy the following two conditions: The level spacings satisfy

$$|E_{n-1}(t) - E_n(t)| < |E_n(t) - E_{n+1}(t)|, \tag{3}$$

and the direct transition is allowed only for nearest-neighbor pairs of levels,

$$\Omega_{mn}(t) \approx 0 \quad \text{unless} \quad m = n \pm 1. \tag{4}$$

These two conditions are satisfied by a broad range of systems subject to open boundary conditions. One important example we will study in the following sections is a 1D topological superconductor whose energy-level structure is shown in Fig. 1(a).

We now develop the generalized KZM. Suppose that initially $|\Psi(t = -\infty)\rangle = |\Phi_0(-\infty)\rangle$. We want to examine the final state $|\Psi(\infty)\rangle$ in the far future. Within the spirit of the KZM [12,13,16], we determine *adiabatic-impulse (AI) crossover points* t_n and t'_n by comparing the *relaxation time*
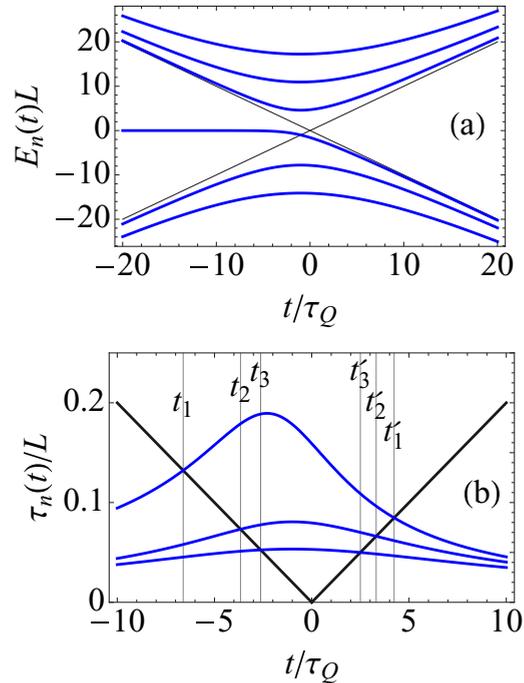

FIG. 1. (Color online) (a) The quasiparticle energy levels (collecting only even-parity modes; see the text) where $E_n(t)$ is labeled in the ascending order of $|E_n|$ and (b) relaxation time scales in a 1D TS of length L and "mass" $M(t)L = t/\tau_Q$, where τ_Q is the quenching time. The AI crossover points t_n and t'_n $(n = 1, 2, \ldots)$ are indicated by thin vertical lines in (b).

scale, $\tau_n(t) = 1/|E_n(t) - E_{n-1}(t)|$, and the time scale for the relative coupling to develop, $M(t)/\dot{M}(t) = t$:

$$\tau_n(t_n) = -\alpha t_n,\ \ \tau_n(t'_n) = +\alpha t'_n\ \ (1 \leqslant n \leqslant N), \tag{5}$$

where $\alpha = O(1)$ is a fitting parameter [19]. Due to the level-spacing structure in Eq. (3), the crossover points are arranged in the order $t_1 < \cdots < t_N < t'_N < \cdots < t'_1$ [see Fig. 1(b)]. Here note that the crossover points may *not* be symmetric about the critical point $(t_n \neq -t'_n)$ [13]. The asymmetry naturally arises in Majorana systems because the zero-energy Majorana mode appears only in one phase during the topological phase transition.

The initial evolution from $t = -\infty$ to t_1 is completely adiabatic and thus $|\Psi(t_1)\rangle = |\Phi_0(t_1)\rangle$. From this moment to t_2, the two levels $E_0(t)$ and $E_1(t)$ become impulsive, but the rest, far away from the two, still remain unpopulated. In the two-level case, the AI approximation assumes that the state remains completely intact: $|\Psi(t_2)\rangle = |\Psi(t_1)\rangle$. A vital difference in the multilevel case is that it violates the probability conservation because even the relatively adiabatic states $|\Phi_n(t_2)\rangle$ $(n \geqslant 2)$ have finite overlaps with $|\Phi_0(t_1)\rangle$ and $|\Phi_1(t_1)\rangle$.

Therefore, we instead choose to "prune" the effective Hamiltonian $K_{mn}(t)$ as follows: Suppose that the first $(r + 1)$ levels $E_0, E_1, \ldots, E_r$ are impulse. Then we ignore the energy differences among impulse levels, $E_m \approx 0$ $(0 \leqslant m \leqslant r)$, and keep only the the dynamic transitions between impulse levels, $\Omega_{mn}(t) \approx 0$ either for $0 \leqslant m \leqslant r < n$ or for $r < m, n$. This

leads to the *pruned* effective Hamiltonian,

$$K_{mn}^{(r)}(t) = \begin{cases} -\Omega_{mn}(t) & (m,n \leqslant r) \\ \delta_{mn} E_n(t) & \text{otherwise,} \end{cases} \quad (6)$$

and the corresponding pruned evolution matrix $U^{(r)}(t,t') \equiv T \exp[-i \int_{t'}^{t} ds\, K^{(r)}(s)]$. The pruning amounts to evolving the impulse levels solely by the dynamic transition matrix Ω_{ij}, while keeping the adiabatic levels intact. Being unitary, $U_{mn}^{(r)}$ preserves the probability. Within the AI approximation, the evolution is thus expected to be governed by

$$U^{(r,s)} \equiv U^{(r)}(t'_r, t'_{r+1}) \cdots U^{(N-1)}(t'_{N-1}, t'_N)$$
$$\times U^{(N)}(t'_N, t_N) U^{(N-1)}(t_N, t_{N-1}) \cdots U^{(s)}(t_{s+1}, t_s). \quad (7)$$

Indeed, getting back to the example, the evolution from t_1 to t_2 is described by $\beta_m(t_2) \approx \sum_n U_{mn}^{(1)}(t_2, t_1)\beta_n(t_1)$. Note that for the two-level case ($N = 1$), this is equivalent to the original AI approximation [12,13]. The same procedure is repeated until t_N to get [recall $\beta_n(-\infty) = \delta_{n0}$]

$$\beta_m(t_N) = [U^{(N-1)}(t_N, t_{N-1}) \cdots U^{(1)}(t_2, t_1)]_{m0}. \quad (8)$$

After the moment $t = t'_N$, the level $E_N(t)$ becomes *relatively adiabatic* again and its occupation probability does not change from $|\beta_N(t'_N)|^2$. The rest evolve impulsively until $t = t'_{N-1}$, when the level $E_{N-1}(t)$ becomes relatively adiabatic. Repeating this approximation until $t = t'_1$, after which the whole evolution becomes adiabatic, one finally obtains the AI approximation for the amplitudes $\beta_m(\infty) \approx U_{m0}^{(m,n)}$. Similarly, starting from a general initial state $|\Phi_n(-\infty)\rangle$ with $n > 0$, one gets the occupation probabilities

$$P_{m|n}(\infty) \approx |U_{mn}^{(m,n)}|^2, \quad P_{m|0}(\infty) \approx |U_{m0}^{(m,1)}|^2,$$
$$P_{0|0}(\infty) \approx |U_{00}^{(1,1)}|^2, \quad P_{0|n}(\infty) \approx |U_{0n}^{(1,n)}|^2, \quad (9)$$

where $m,n > 0$. Equation (9) is called the *conserving KZM* for the multilevel system as it conserves the probability, $\sum_m P_{m|n}(\infty) = 1$. It generalizes the KZM for two-level systems, and the calculation involves simple procedures requiring only instantaneous eigenvectors.

Although the expression (9) requires only instantaneous eigenvectors at discrete times, one still needs to calculate the time-ordered exponential function of the matrix $\Omega(t)$. As we will see now, in many cases it can be avoided. For a large system, the AI crossover points are closely packed and each factor in (9) can be approximated by

$$U_{ij}^{(r)}(t + \eta, t) \approx \begin{cases} \delta_{ij} + i\eta\Omega_{ij}(t) & (i,j \leqslant r) \\ \delta_{ij}[1 - i\eta E_j(t)] & \text{otherwise,} \end{cases} \quad (10)$$

up to $O(\eta^2)$. When Eq. (10) is substituted into Eq. (9), due to Eq. (4), only the subpart $\delta_{ij} + i\eta\Omega_{ij}(t)$ ($i,j \leqslant r$) of each matrix $U^{(r)}(t + \eta, t)$ contributes to the product; hence, $U^{(r)}(t + \eta, t)$ in Eq. (9) can be replaced safely with $1 + i\eta\Omega(t) \approx W(t + \eta, t)$ up to $O(\eta^2)$. Then the probability reduces to [recall that $W_{mn}(t', t) = \langle \Phi_m(t')|\Phi_n(t)\rangle$]

$$P_{m|n}(\infty) \approx |\langle \Phi_m(t'_m)|\Phi_n(t_n)\rangle|^2, \quad (11a)$$

$$P_{m|0}(\infty) \approx |\langle \Phi_m(t'_m)|\Phi_0(t_1)\rangle|^2, \quad (11b)$$

$$P_{0|n}(\infty) \approx |\langle \Phi_0(t'_1)|\Phi_n(t_n)\rangle|^2, \quad (11c)$$

$$P_{0|0}(\infty) \approx |\langle \Phi_0(t'_1)|\Phi_0(t_1)\rangle|^2, \quad (11d)$$

where $m, n > 0$. This approximation, which we call the *nonconserving KZM* for the multilevel system, drastically simplifies the calculation of $P_{m|n}$ which demands only the overlap integrals of instantaneous eigenvectors at different times. The caveat is that it violates the probability conservation (hence the name "nonconserving"), $\sum_m P_{m|n}(t) < 1$, as it involves eigenstates $|\Phi_m(t'_m)\rangle$ at different times for different levels. The amount of violation, $\varepsilon = 1 - \sum_m P_{m|n}(\infty)$, gives a convenient estimate of the error. The result (11) implies that given the initial state $|\Phi_n(-\infty)\rangle$, the system essentially remains impulse from t_n to t'_m. Indeed, the nonconserving KZM essentially assumes that the part associated with the relative impulse levels remains completely intact [see the discussion above Eq. (6)]. However, the derivation of the nonconserving KZM via the conserving KZM using the pruned evolution matrix $U_{mn}^{(r)}$ paves a way to further generalizations of the KZM for systems with more complicated level and coupling structure. Moreover, in practice, the violation does not affect its accuracy so much, as demonstrated below.

III. TOPOLOGICAL SUPERCONDUCTOR

Now we apply the generalized KZM developed above to study the dynamics of topological phase transitions. We consider a particular example, namely, 1D TS. 1D TS is a simple but important prototype for the study of the dynamical aspects of Majorana fermion.

A 1D TS of length L is described by the tight-binding Hamiltonian of $N_L = L/a$ spinless fermions with a being the lattice constant [20],

$$\hat{H}(t) = \frac{w}{2} \sum_{j=1}^{N_L-1} [\hat{c}_j \hat{c}_{j+1} - \hat{c}_j^\dagger \hat{c}_{j+1} + \text{H.c.}] - \mu(t) \sum_{j=1}^{N_L} \hat{c}_j^\dagger \hat{c}_j. \quad (12)$$

Here, for simplicity, we take the Ising limit in which the p-wave superconducting order parameter Δ is equal to the hopping amplitude w. In the quenching process, the chemical potential $\mu(t)L = w(t/\tau_Q + L)$ [21] is ramped up from 0 to ∞ through the transition point $\mu = w$ at $t = 0$. The process drives the system from the topological ($|\mu| < w$) to trivial ($|\mu| > w$) phase.

In the continuum limit, Eq. (12) is reduced to the Dirac Hamiltonian

$$\hat{H}(t) = \frac{1}{2} \int dx\, \hat{\Psi}^\dagger(x) H(x,t)\hat{\Psi}(x), \quad \hat{\Psi} = \begin{bmatrix} \hat{\psi} \\ \hat{\psi}^\dagger \end{bmatrix}, \quad (13)$$

with $H(x,t) = M(x,t)v_s^2\tau_z - i\hbar v_s\tau_x\partial_x$, where τ_x, τ_y, τ_z are the Pauli matrices in the particle-hole space, $\hbar v_s = a\Delta$, and $Mv_s^2 = \mu - w$. Hereafter, we use the unit system such that $\hbar = v_s = a = 1$ (note that $N_L = L$). The position-dependent "mass" $M(x,t)$ accounts for the spatially inhomogeneous regions of the TS. We are particularly interested in the case [22,23]

$$M(x,t) = \begin{cases} \infty & (|x| > L/2) \\ M(t) & (|x| \leqslant L/2) \end{cases}. \quad (14)$$

When $M(t) < 0$, there exist two zero-energy Majorana fermions localized at $x = \pm L/2$ [3]. In the continuum limit, we consider the quenching of the form $M(t)L = t/\tau_Q$ [21].

For simplicity, we mostly discuss the dynamics in terms of the continuum model; qualitative features are the same.

A. Single-particle states

We start with the single-particle Dirac equation

$$H(x,t)\Phi_n(x,t) = E_n(t)\Phi_n(x,t). \quad (15)$$

It has two important symmetries: the space inversion and the particle-hole symmetry. The inversion symmetry allows us to choose a solution to be a parity eigenstate and subject to the boundary conditions

$$\Phi_n(L/2,t) = \pm\tau_z\Phi_n(-L/2,t) = \begin{bmatrix} 1 \\ i \end{bmatrix}, \quad (16)$$

where the sign $\pm$ corresponds to the even/odd parity under the space inversion. Because of the particle-hole symmetry, if $\Phi_n(x,t)$ is a solution of the Dirac equation with energy $E_n(t)$, then its charge conjugation partner $\tau_x\Phi_n^*(x,t)$ is also a solution but with energy $-E_n(t)$. Further, if $\Phi_n(x,t)$ has a definite (even or odd) parity, then $\tau_x\Phi_n^*(x,t)$ has the opposite parity. Hence it suffices to count only, say, even-parity solutions. Hereafter, we reserve the notation $\Phi_n(x,t)$ for the even-parity modes,

$$\Phi_n(x,t) = \begin{bmatrix} \sin(k_n L/2)\cos(k_n x) \\ i\cos(k_n L/2)\sin(k_n x) \end{bmatrix}, \quad (17)$$

with $k_n(t)$ satisfying $\tan(k_n L) = -k_n/M$. Odd-parity modes are referred to by $\tau_x\Phi_n^*(x,t)$. The mode $\Phi_n(x,t)$ has energy $E_n(t) = (-1)^{n-1}\sqrt{M^2(t) + k_n^2(t)}$ with $n = 0,1,2,\dots$ in the increasing order of $|E_n|$, whose time dependence is illustrated in Fig. 1(a). Of particular importance is the *zero mode*, $\Phi_0(x,t)$, whose energy $E_0(t) \approx M(t)/\cosh[M(t)]$ is exponentially small for $M(t)L < -1$ and physically responsible for the Majorana modes localized at the interfaces (k_0 is purely imaginary). The energy levels $E_n(t)$ and the dynamical transitions $\Omega_{mn}(t)$ between them in 1D TS [Fig. 1(a)] satisfy the conditions (3) and (4), and hence we can apply the generalized KZM developed above.

In passing, the property (4) casts a sharp contrast between the OBC and PBC [14]. Under the PBC, momentum is conserved and transitions in 1D TS occur only between modes with opposite momenta k and $-k$: $\Omega_{kk'} = 0$ unless $k + k' = 0$. Therefore, the dynamical model is essentially a two-level system [14,18] and the KZM for two-level systems is enough. Of course, in the thermodynamic limit, the boundary condition does not make a difference in bulk states. However, the Majorana states at the boundaries do not have a counterpart under the PBC and cause the inherently multilevel dynamics.

B. Quasiparticle excitations

Let us now consider the dynamics of the *many-body* Hamiltonian and apply the generalized KZM developed above. The full many-body dynamics is intimately related to the single-particle dynamics. To see the connection, denote the quasiparticle operator for the mode $\Phi_n(x,t)$ and $\tau_x\Phi_n^*(x,t)$ by $\hat{a}_n(t)$ and $\hat{b}_n(t)$, respectively. Obviously, $a_n^\dagger(t) = b_n(t)$. In terms of these, the many-body Dirac Hamiltonian (13) reads $\hat{H}(t) = \sum_{n=0}^\infty E_n(t)[\hat{a}_n^\dagger(t)\hat{a}_n(t) - 1/2]$. The actual dynamics is governed by the Heisenberg operators $\tilde{a}_n(t)$, related to the

instantaneous eigenoperators $\hat{a}_n(t)$ by $\tilde{a}_n(t) = \hat{V}^\dagger(t)\hat{a}_n(t)\hat{V}(t)$, where $\hat{V}(t)$ is the many-body time-evolution operator $\hat{V}(t) = T\exp[-i\int_{-\infty}^t ds\,\hat{H}(s)]$. They satisfy the Heisenberg equation of motion,

$$i\frac{d}{dt}\tilde{a}_m(t) = \sum_n K_{mn}(t)\tilde{a}_n(t), \quad (18)$$

or, equivalently,

$$\tilde{a}_m(t) = \sum_n U_{mn}(t,t_0)\tilde{a}_n(t_0), \quad (19)$$

with $U(t,t') = T\exp[-i\int_{t'}^t ds\,K(s)]$. Equations (18) and (19) illustrate that the effective single-particle Hamiltonian K and the corresponding time-evolution operator U [see also Eq. (1)] establish the connection between the many-body and single-particle dynamics.

Initially ($t_0 = -\infty$), the system is prepared in its instantaneous many-body *ground state* $|G(t_0)\rangle$, which is the vacuum of all *positive-energy modes*, $\Phi_{2j+1}(x,t_0)$ and $\tau_x\Phi_{2j}^*(x,t_0)$,

$$\hat{a}_{2j+1}(t_0)|G(t_0)\rangle = \hat{b}_{2j}(t_0)|G(t_0)\rangle = 0, \quad (20)$$

and in which all *negative-energy modes*, $\Phi_{2j}(x,t_0)$ and $\tau_x\Phi_{2j+1}^*(x,t_0)$, are occupied,

$$\langle G(t_0)|\hat{a}_{2j}^\dagger(t_0)\hat{a}_{2j}(t_0)|G(t_0)\rangle$$
$$= \langle G(t_0)|\hat{b}_{2j+1}^\dagger(t_0)\hat{b}_{2j+1}(t_0)|G(t_0)\rangle = 1. \quad (21)$$

We examine the number of excited quasiparticles $\mathcal{N}$ in the far future ($t = \infty$). $\mathcal{N}$ is directly related to the number of topological defects created by the quenching process across the critical point [14]. Due to the initial conditions (20) and (21), the occupancy of *positive-energy modes*, $\tau_x\Phi_{2i}^*(x,\infty)$ and $\Phi_{2i+1}(x,\infty)$, are given by $\sum_{j=0}^\infty P_{2i|2j+1}$ and $\sum_{j=0}^\infty P_{2i+1|2j}$, respectively. The total number $\mathcal{N}$ of *excited* quasiparticles is therefore given by $\mathcal{N} = \sum_{i,j=0}^\infty [P_{2i|2j+1} + P_{2i+1|2j}]$.

The contribution of the Majorana mode, $\mathcal{N}_0 \equiv \sum_{m\in\text{odd}} P_{m|0}$, is of particular interest as it is known to defy the traditional KZM [6,7]. It is stressed that the Majorana-mode contribution $\mathcal{N}_0$ can be measured experimentally [24]: Consider two different quenching procedures, with one starting from the ground state $|G(t_0)\rangle$ and the other starting with the Majorana mode excited $\hat{b}_0^\dagger(t_0)|G(t_0)\rangle = \hat{a}_0(t_0)|G(t_0)\rangle$. We find that $\mathcal{N}_0$ is related to the difference $\Delta\mathcal{N}$ in $\mathcal{N}$ for these two processes by $\mathcal{N}_0 = (1 - \Delta\mathcal{N})/2$ since $\Delta\mathcal{N} = \sum_{m\in\text{even}} P_{m|0} - \sum_{m\in\text{odd}} P_{m|0}$ and $\sum_{m\in\text{odd}} P_{m|0} + \sum_{m\in\text{even}} P_{m|0} = 1$.

Figure 2 shows $\mathcal{N}$ and $\mathcal{N}_0$ as a universal function of L/τ_Q for both the continuum and lattice models. It demonstrates that the generalized (both conserving and nonconserving) KZM predictions agree well with the exact results [25]. More importantly, it reveals three more prominent features of the generalized KZM distinguished clearly from the traditional KZM: (i) The agreement remains good far beyond the traditional KZM scaling region. The celebrated scaling behavior $\mathcal{N} \sim \sqrt{L/\tau_Q}$ (i.e., $L\sqrt{\tau_0/\tau_Q}$ in the natural units and for the traditional L-independent definition of τ_Q [21]) is known [14,16,26] to be valid only for relatively fast quenching [Figs. 2(a) and 2(b)]. For slower quenching, the exact dynamics and the traditional KZM do not agree any longer. On the contrary, the generalized KZM works remarkably well even for
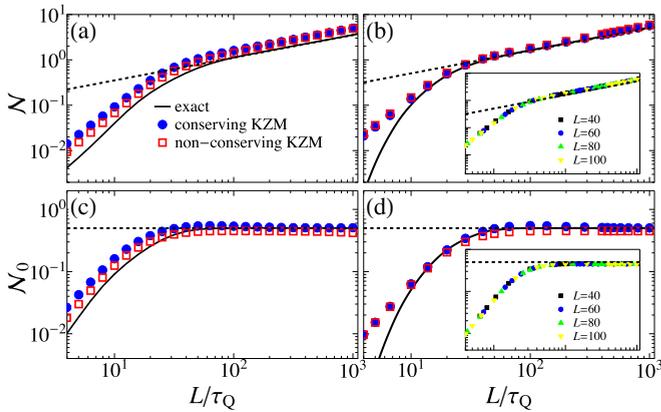
FIG. 2. (Color online) (a),(b) The total number $\mathcal{N}$ of defects and (c),(d) the contribution $\mathcal{N}_0$ of the Majorana state Φ_0 in the (a),(c) continuum model and (b),(d) lattice model. The black solid line, blue filled circle, and red empty square are the results of the exact calculation, conserving KZM, and nonconserving KZM, respectively. The dashed line in (a) and (b) indicates the traditional KZM scaling $\mathcal{N} \sim \sqrt{L/\tau_Q}$. (a),(c) $N = 13$. (b),(d) $L = 100$. Insets: The finite-size scaling for different sizes (calculated by the nonconserving KZM).

slow quenching [Figs. 2(a) and 2(b)]. (ii) The Majorana-mode contribution $\mathcal{N}_0$ completely defies the traditional KZM, as first pointed out in Refs. [6,7], whereas it is well explained by the generalized KZM [Figs. 2(c) and 2(d)]. Since the Majorana mode plays a key role in the topological PT, understanding its dynamics is vital. Its inherent bound-state character and multilevel structure are efficiently captured by the generalized KZM. (iii) The saturation of $\mathcal{N}_0$ to 1/2 for fast quenching [Figs. 2(c) and 2(d)] is intimately related to the multilevel structure and the localization of the Majorana state, and Eq. (11b) provides a simple explanation: Let τ_Q^* be the quenching time such that $M(t_1)L = -1$; $L/\tau_Q^* \approx 10$. For $\tau_Q \ll \tau_Q^*$, $M(t_1)L \ll -1$. It means that for such fast quenching, the Majorana mode $\Phi_0(x,t_1)$ is well localized and its overlap with any bulk state $\Phi_m(x,t_m')$ is the same, independent

of m. Hence, $\mathcal{N}_0 = \sum_{m \in \text{odd}} |\langle \Phi_m(t_m')|\Phi_0(t_1)\rangle|^2 \approx 1/2$ since $\sum_{m \in \text{odd}} P_{m|0} \approx \sum_{m \in \text{even}} P_{m|0}$ in this condition. For slower quenching ($\tau_Q \gg \tau_Q^*$), on the other hand, $M(t_n)L > -1$ for all n; namely, by the time the impulse region is reached, the state $|\Phi_0(t_1)\rangle$ loses the Majorana character and the above argument does not hold any longer.

We finally note that Ref. [7] studied (numerically) a different parameter regime of the same system (12). They kept $\mu = 0$ and varied w from $-\Delta$ to Δ. However, the dynamics is essentially the same. With $\mu = 0$, Eq. (12) is decomposed into two decoupled Majorana chains that have opposite effective Dirac masses, $M(t) = w - |\Delta|$ and $-M(t)$, but are identical otherwise. Explicit calculation indeed reproduces their results.

IV. CONCLUSION

In conclusion, we have developed a generalized KZM, which agrees well with the exact dynamics in a wide range of quenching rate. In particular, it successfully describes the contribution of the Majorana mode to the quenching-induced topological defects, which is essential in the dynamics of the topological PT. While in this work we have applied the generalized KZM only to a specific model such as the 1D topological superconductor, we believe that it can be applied to many diverse systems. The only condition for our KZM to work is that the system has the multilevel structure; more specifically, that the level spacings and the dynamical transitions follow Eqs. (3) and (4), respectively. Since the multilevel structure appears frequently in finite-size systems, our KZM can be used to study the effect of boundaries in the quench process. More importantly, our scheme provides an intuitive and systematic method to capture the physics of the quench in terms of wave-function overlaps (11).

ACKNOWLEDGMENTS

[1] M. Z. Hasan and C. L. Kane, Rev. Mod. Phys. **82**, 3045 (2010).

[2] X.-L. Qi and S.-C. Zhang, Rev. Mod. Phys. **83**, 1057 (2011).

[3] S.-Q. Shen, *Topological Insulators*, Vol. 174 of Springer Series in Solid-State Sciences (Springer, Berlin, 2012).

[4] E. Perfetto, Phys. Rev. Lett. **110**, 087001 (2013).

[5] W. DeGottardi, D. Sen, and S. Vishveshwara, New J. Phys. **13**, 065028 (2011).

[6] A. Bermudez, D. Patanè, L. Amico, and M. A. Martin-Delgado, Phys. Rev. Lett. **102**, 135702 (2009).

[7] A. Bermudez, L. Amico, and M. A. Martin-Delgado, New J. Phys. **12**, 055014 (2010).

[8] T. W. B. Kibble, J. Phys. A **9**, 1387 (1976).

[9] T. Kibble, Phys. Rep. **67**, 183 (1980).

[10] W. H. Zurek, Nature (London) **317**, 505 (1985).

[11] W. H. Zurek, Phys. Rep. **276**, 177 (1996).

[12] B. Damski, Phys. Rev. Lett. **95**, 035701 (2005).

[13] B. Damski and W. H. Zurek, Phys. Rev. A **73**, 063405 (2006).

[14] J. Dziarmaga, Phys. Rev. Lett. **95**, 245701 (2005).

[15] J. Dziarmaga, W. H. Zurek, and M. Zwolak, Nat. Phys. **8**, 49 (2012).

[16] W. H. Zurek, U. Dorner, and P. Zoller, Phys. Rev. Lett. **95**, 105701 (2005).

[17] R. Vasseur, J. P. Dahlhaus, and J. E. Moore, Phys. Rev. X **4**, 041007 (2014).

[18] Y. N. Demkov and V. N. Ostrovsky, J. Phys. B **28**, 403 (1995).

[19] It was found that $\alpha = \pi/2$ in the two-level case in [13].

[20] A. Y. Kitaev, Phys. Usp. **44**, 131 (2001).

[21] Here we have adopted L-dependent τ_Q to be consistent with the relativity convention, where time t and length L have the same dimension. Replacing $\tau_Q \to \tau_Q/L$ recovers the traditional L-independent definition of τ_Q such as in [6,7,14,16].

[22] L. Fu and C. L. Kane, Phys. Rev. Lett. **100**, 096407 (2008).

[23] For our purposes, it suffices that $M(x,t) > 0$ for $|x| > L/2$, but for simplicity we put it to be infinitely large. One physical realization was suggested in [22]. Below we also discuss Kitaev's original lattice model, which is closer to realistic systems.

[24] An equivalent way to get the Majorana-mode contribution $\mathcal{N}_0$ is preparing the system initially in the *Bogoliubov vacuum* $|\Omega(t_0)\rangle$ [6,7]. Unlike the *ground state* $|G(t_0)\rangle$, which is the vacuum of only positive-energy states, $|\Omega(t_0)\rangle$ is the vacuum of all positive- and negative-energy modes. Accordingly, its energy is much higher than the ground-state energy, by the amount $\sum_{j=0}^{\infty}(|E_{2j}| + E_{2j+1}) \to \infty$. It may not be easy to prepare the system in such an initial state.

[25] We found that the choice of the fitting parameter α, as long as it is $\sim O(1)$, does not alter the qualitative behavior of $\mathcal{N}$ and $\mathcal{N}_0$ and that the quantitative dependence of $\mathcal{N}$ and $\mathcal{N}_0$ on other parameters remains quite immune to the tuning of α as long as $\mathcal{N} \gtrsim 1$.

[26] J. Dziarmaga, Adv. Phys. **59**, 1063 (2010).